

Braking Process in Automobiles: Investigation of the Thermoelastic Instability Phenomenon

M. Eltoukhy and S. Asfour

*Department of Industrial Engineering, College of Engineering, University of Miami
USA*

1. Introduction

During the braking action, the kinetic energy produced at the wheel is transformed into heat energy, which doesn't dissipate fast enough into the air stream from the brake to the brake disk; as a result, the thermal conductivity plays a critical role in handling such heat generated.

Thermal judder, which is a result of non-uniform contact cycles between the pad and the disk brake rotor, which is primarily an effect of the localized Thermo-Elastic Instabilities (TEI) at the disk brake rotor surface. Localized TEI act at the friction ring surface generating intermittent hot bands around the rubbing path which may in turn leads to the development of so-called hot spots.

In this chapter a case study regarding a transient analysis of the thermoelastic contact problem for disk brakes with frictional heat generation, performed using the finite element analysis (FEA) method is described in details. The computational results are presented for the distribution of the temperature on the friction surface between the contacting bodies (the disk and the pad).

Also, the influence of the material properties on the thermoelastic behavior, represented by the maximum temperature on the contact surface is compared among different types of brake disk materials found in the literature, such as grey cast iron (grey iron grade 250, high-carbon grade iron, titanium alloyed grey iron, and compact graphite iron (CGI)), Aluminum metal matrix composites (Al-MMC's), namely Al₂O₃ Al-MMC and SiC Al-MMC (Ceramic brakes).

This comparison was performed in order to improve the conceptual design of the disk brakes. The results obtained from the suggested model are compared with actual measurements obtained from experiments performed by Cueva et al.(2003). The FEA results were in excellent agreement with the actual measurements reported by Cueva et al. for all of the suggested brake disk materials.

A comparison between two different brake disk rotor designs was performed as well in order to study the effect of the perforated brake disks on the maximum temperature, the temperature distribution, and the heat flux produced under the same braking conditions.

1.1 Braking process

By pressing the brake pedal the car transmits the force from the driver's foot to the brakes through a fluid then the brakes transmit the force to the tires by friction, as a result the tires transmit that force to the road using friction as well. Figure 1 depicts a simple braking system. One important conclusion can be drawn from the shown figure, that the force applied by the driver is multiplied by a certain factor (about 36) through two mechanisms, first is through the distance from the cylinder to the pivot, and second is the difference in the brake cylinder compared to the pedal cylinder.

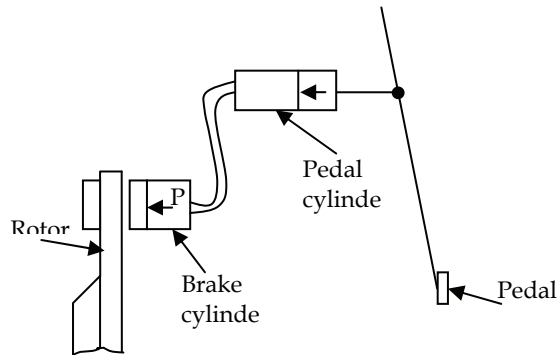


Figure 1. Simple braking system

In this chapter, the main type of brakes that are investigated is the single-piston floating calliper disk brakes. Figure 2 shows the main components of that type of disk brakes, which are; the calliper, the rotor, and the pads.

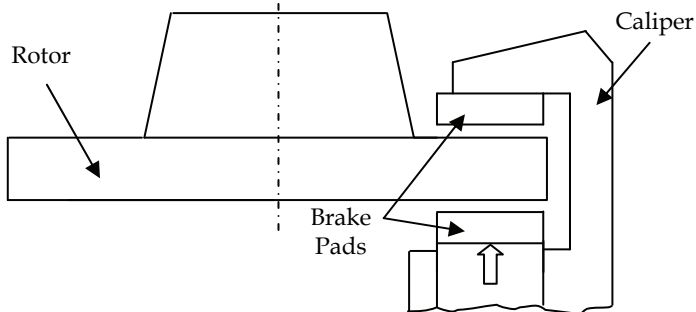


Figure 2. Disk brake components

2. Vehicles Dynamics

Load transfer refers to the shifting of weight around a vehicle during acceleration. This includes braking, and deceleration. It is important to differentiate between two terms that are used, in the literature, interchangeably although they are not synonymous; load transfer and weight transfer. The difference between the two terms is that, load transfer is an imaginary shift in the weight due to acceleration while the weight transfer involves the actual movement of the vehicle's centre of gravity relative to the wheel axes. These two

terms are used to describe the redistribution of the total vehicle load among the different tires. The traction at each wheel to accelerate the vehicle in such direction is affected by load transfer; if the load is equally distributed among the tires then more total traction will be available.

The main forces that accelerate a vehicle occur at the tires' contact patches. Since these forces are not directed through the vehicle's CoG, one or more moments are generated whose forces are the tires' grip forces, the other one, which is equal in magnitude but opposed in direction, is the mass inertia located at (CoG). These moments cause variation in the load distributed among the tires.

According to Newton's second law written for the x-direction (see Fig.3.), the braking forces can be written as:

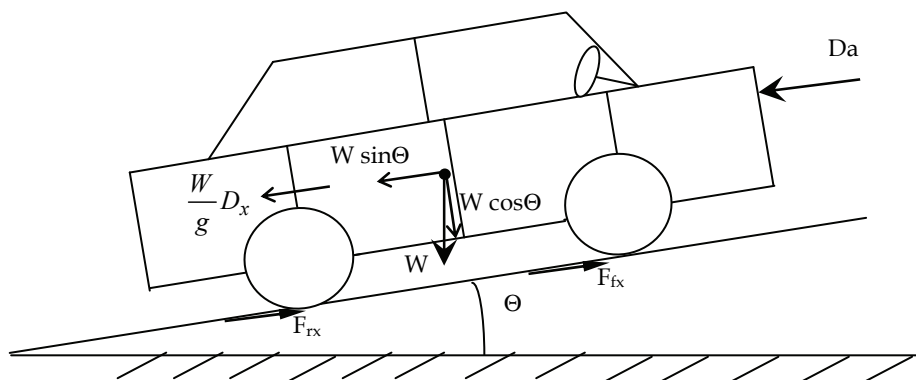


Figure 3. The major forces acting on the vehicle

$$\sum F_x = M \cdot a_x = -\frac{W}{g} D_x = -F_{fx} - F_{rx} - D_a - W \sin \Theta \quad (1)$$

Where:

F_x : Forces in the x-direction

M: Mass

a_x : Acceleration in the x-direction

W: Body weight

g: Gravitational acceleration

D_x : Linear deceleration

F_{fx} : Front braking force

F_{rx} : Rear braking force

D_a : Aerodynamic drag

Θ : Uphill grade

A number of important terms related to the braking performance are described below; these terms are constant deceleration, rolling resistance, and aerodynamic drag.

Constant deceleration

Based on the assumption that the forces acting on the vehicle will remain constant during the braking application, and according equation (1), the following can be obtained:

$$D_x = \frac{F_{tx}}{M} = -\frac{dV}{dt} \quad (2)$$

Where:

F_{tx} : The total deceleration forces in the x-direction

V: Velocity

Assume that the vehicle initial velocity is V_1 and the final velocity is V_2 , and the time needed for the velocity to be changed from V_1 to V_2 is T . By integrating equation (2) the following will be obtained:

$$\int_{V_1}^{V_2} dV = -\frac{F_{tx}}{M} \int_0^T dt \quad (3)$$

$$V_1 - V_2 = \frac{F_{tx}}{M} T \quad (4)$$

In case of complete stop ($V_2=0$), and according to the relationship between distance and velocity, the distance (X_s) and time (T_s) needed for the vehicle to reach complete stop can be determined as follows;

$$X_s = \frac{V_1^2}{2D_x} \quad (5)$$

$$T_s = \frac{V_1}{D_x} \quad (6)$$

Rolling Resistance

This resistance helps the brakes stopping the vehicles; a typical value to this type of resistance is 0.3 ft/sec².

Aerodynamic Drag

Depends on the dynamic pressure, and its proportional to the speed squared. This type of drag is to be neglected at low speeds.

3. Thermo-Elastic Instability (TEI)

As shown before, the brake pads squeeze against the rotor, thus friction between the pads and the disc slows the vehicle down. The brakes then have to remove the kinetic energy from the vehicle, and in turn it converts it into heat.

Frictional heat generated due to friction as well as the thermoelastic deformation alters the contact pressure distribution between the two contacting surfaces, as a result and above a certain speed (critical speed), hot spots are observed due to the localization of heat generated (Barber, 1969 and Kennedy & Ling, 1974). Hot spots can be a source of frictional vibrations known as hot judder (Zagrodzki, 1990).

Once the brake pads come in contact with the sinusoidal surface during braking severe vibrations are induced. Thermal stresses due to high temperatures may induce a number of unfavorable conditions such as surface cracks and permanent distortions. Frictional heating, thermal deformation and elastic contact in sliding contact systems affect the contact pressure and temperature on the friction surfaces.

Accordingly, TEI imposes design constraints on systems such as automotive brakes and clutches, thus it has been investigated by a number of researchers. The mechanism of TEI in sliding systems involving frictional heating was first explained by Barber (1967), who observed experimentally the resulting hot spots in railway brakes. Kennedy and Ling (1974) were first to obtain numerical simulations of thermomechanical behaviours occurring in aircraft-type multidisk brakes.

Zagrodzki et al.(1990) implemented a transient finite element simulation for the 2-D thermoelastic contact problem of a stationary layer between two sliding layers with frictionally excited thermoelastic instability using the Petrov–Galerkin algorithm. Choi and Lee developed a finite element model for an axisymmetric coupled thermoelastic contact problem simulating a disk brake and investigated the TEI phenomena of disk brakes during the drag braking process.

3.1 Thermo-Mechanical Distortion of Disk Rotors

Due to the non equilibrium thermal expansion of the rotor, increase in the thermal deformation takes place which in turn results in further localization of the friction contact. Thermal deformation contributes to a number of geometrical distortions in the disk rotor, it may lead to warped friction ring (thermal buckling), and also it may result in disk coning (Sterne, 1989). The thermal judder phenomenon may also lead to radial cracking as a result of the high generated compressive hoop stresses and / or plastic flow of the rotor surface.

The pattern of surface temperature variation in the radial direction of the friction ring being seen to be the same for both sides of the friction ring. Lateral / axial, Side-face RunOut of the disc brake rotor has also been shown to make some contribution to the phenomenon of hot spotting and thus to thermal judder (Inoue, 1986). As a result of the high thermal stresses involved, permanent deformations of the rotor geometry may also persist beyond the braking applications where judder phenomena are experienced. Also, the occurrence of hot spots places high thermal load on the rotor material and may lead to phase transformations within the cast iron.

A number of approaches have been suggested to help solving the thermal judder problem, these approaches have in common that they try improving the distribution of the heat generated, some of the solutions suggested includes improving the thermal conductivity and specific heat capacity of the rotor material, and reducing the friction contact arc length.

4. Case study

4.1 Problem definition

During the braking action, the kinetic energy produced at the wheel is transformed into heat energy, which doesn't dissipate fast enough into the air stream from the brake to the brake disk, because of that, one of the disk brake material properties; the thermal conductivity plays a critical role in handling such friction heat generated. Thermal judder occurs as a result of non-uniform contact cycles between the pad and the disk brake rotor, which is primarily an effect of the localized Thermo-Elastic Instabilities at the disk brake rotor surface.

Localized TEI act at the friction ring surface generating intermittent hot bands around the rubbing path which may in turn leads to the development of so-called hot spots (Eggleston, 2000).The mechanism of the TEI phenomena taking place during the braking process has been of interest to many researchers (Lee, 2000; Jang & Khonsari, 2003; Lee & Brooks, 2003; Dufrenoy, 2004; Jacobsson, 2003).

The suggested FEA model simulates the braking action by investigating both the thermal and elastic actions occur during the friction between the two sliding surfaces (the disk brake and the pad). The TEI phenomenon of disk brakes is investigated during repeated brake cycles. Also, the influence of the material properties on thermoelastic behaviours is investigated to facilitate the conceptual design of the disk brake system.

4.2 Methodology

In this case study (Based on the work done by Eltoukhy et al., 2006) an assumption has been made that the thermomechanical phenomenon of each disk are in symmetry about the disk's mid-plane. Also, the wear action taking place during the braking process, resulting from the friction between the disk brake and the pad, is assumed to be so small and thus to be neglected in the analysis.

The simulation was divided into two parts: thermal and elastic. During the analysis, the braking parameters are set to certain values based on the values that have been stated in the literature. These parameters include the rotational speed of the disk brake and the cycle of the pressure applied. Figure 4 depicts the change in pressure during the braking process, and the time period of the different phases of, braking, dragging, and release.

As shown in figure 4, it is assumed that the pressure will first increase linearly until it reaches the maximum value P_{max} (point A to B) within a period of time depends on the vehicle's dynamics, then the pressure remains constant (point B to C), then it drops to zero (point D).

The governing equation for the transient heat transfer problem is:

$$\rho C \frac{\partial T}{\partial t} + \nabla \cdot (-k \nabla T) = Q - \rho C_p u \cdot \nabla T \tag{8}$$

Where:

- ρ : Density
- C : Heat capacity
- T : Temperature
- u : Velocity field
- k : Thermal conductivity
- Q : Heat source or heat sink
- C_p : Specific heat capacity

While the governing equation for the elastic problem is:

$$\rho \frac{\partial^2 u}{\partial t^2} - \nabla \cdot c \nabla u = K \tag{9}$$

Where, K is the force vector.

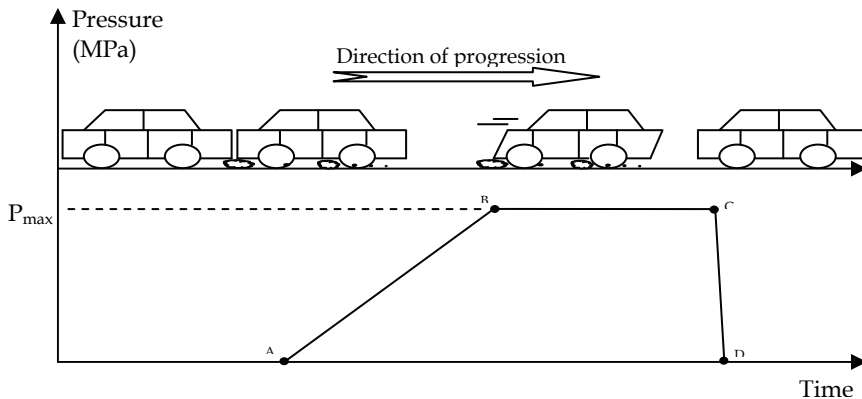


Figure 4. The change in the applied Pressure during the braking process

Boundary Conditions

Figure 5 shows the boundary conditions assumed during the simulation of the heat transfer problem.

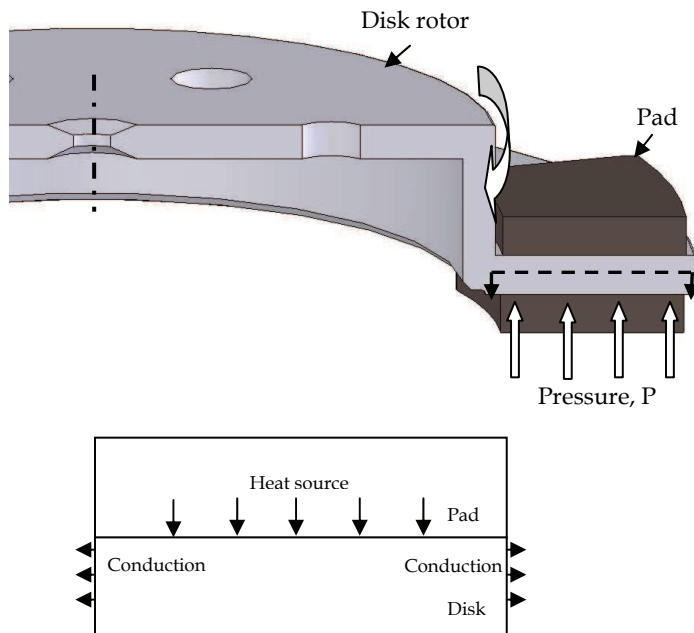


Figure 5. Heat transfer boundary conditions

The boundary conditions stated for the elastic problem are shown in figure 6.

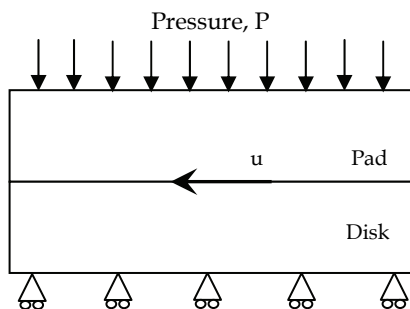


Figure 6. Elastic problem boundary conditions

The objective of this case study is to simulate the thermoelastic phenomenon taking place during the braking process. In addition, a comparison of the thermal behavior of the different brake disk materials found in the literature. Another comparison is performed between two different brake disk designs (perforated and the notched disks), in which the temperature distribution and the heat flux developed under the same operating condition was conducted.

The comparison performed between different types of brake disk rotor materials reported in the literature, was namely between grey cast iron (grey iron grade 250, high-carbon grade iron, titanium alloyed grey iron, and compact graphite iron (CGI)), Aluminum metal matrix composites (Al-MMC's), namely Al₂O₃ Al-MMC and SiC Al-MMC (Ceramic brakes). The comparison was performed in order to improve the conceptual design of the disk brakes. The results obtained from the model were compared with actual measurements obtained from experiments performed by (Cueva et al., 2003). Also, a comparison of the different brake disk designs was performed in order to study the effect of the perforated brake disks on the maximum temperature, temperature distribution, and the heat flux produced as well, under the same braking conditions.

The elastic problem was simulated in order to investigate the mechanical action taking place at the disk's contact surface during the braking process, the deformation obtained from the elastic problem was relatively small (200 μm).

4.3 Results

The developed finite element analysis model contains a total of 278 elements and 597 degrees of freedom, while the time step used during the numerical computation was 0.01sec. The initial temperature used during the simulation was set as 20 °C.

Figure 7 depicts one of the typical temperature distributions developed using the suggested finite element analysis model. It's shown how the temperature increases further from the centre of the disk rotor to the point of the maximum temperature within the contact area between the disk and the pad, and then it decreases.

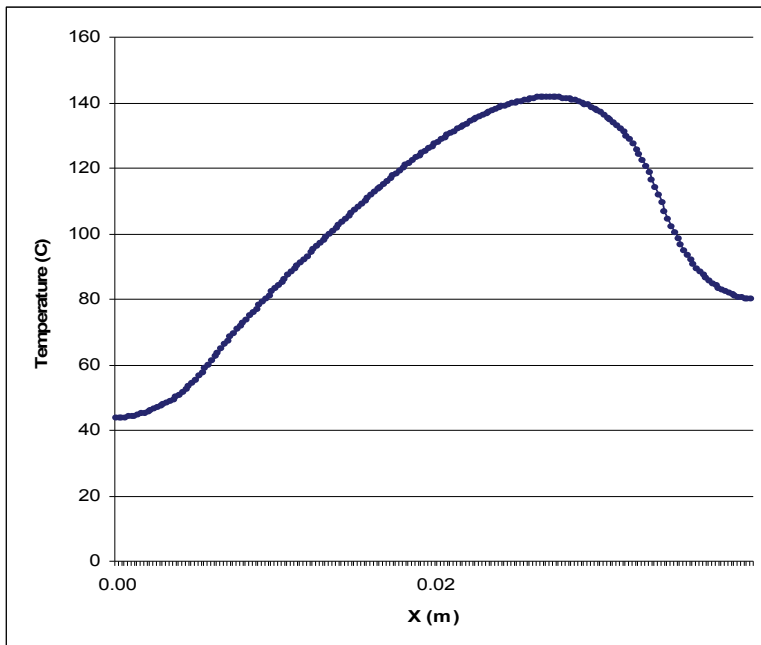


Figure 7. Typical temperature distribution produced during the braking process

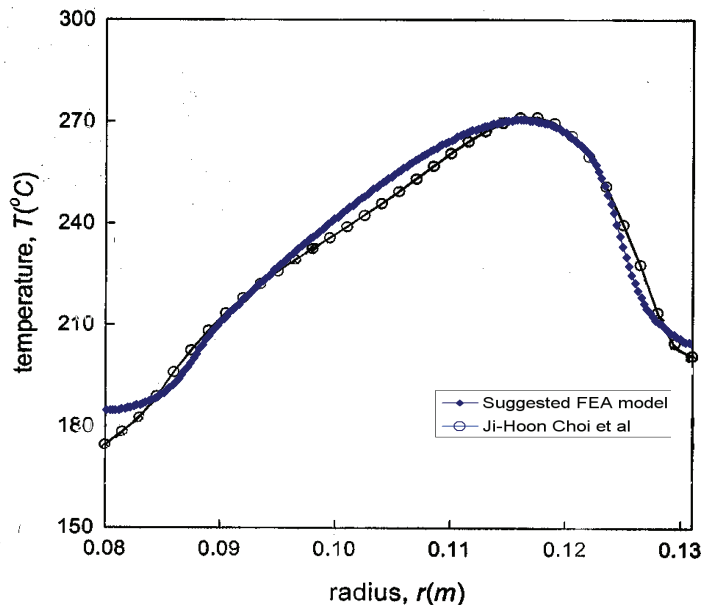


Figure 8. Comparison between the temperature distribution plot obtained by Choi et al. (2004) and the suggested model output

A comparison between the produced temperature distribution using the proposed finite element analysis model and the distribution presented by Choi et al. (2004), under the same operating conditions, is shown in figure 8. A very close fit between the proposed model and the one developed by Choi et al. was obtained.

Figure 9.a presents a 3D plot of the temperature distribution along the contact surface during and after the braking action (time steps 1 to 10 s). While figure 9.b shows the line plot of the temperature distribution at each time step during the same periods of time. As shown in the figure, the temperature produced increases till it reaches its maximum value at the time step 4s, then it decreases after the applied pressure is released.

The temperature distributions during the braking process at 4 different time instants (1,3,4, and 5 seconds) are shown in figure 10 for one of the brake disk materials investigated, namely GI250.

As shown in the figure, at time step 5sec. localization of the heat generated is noticed, which is represented by the dark area on the contact surface, resulted in the development of a hot spot.

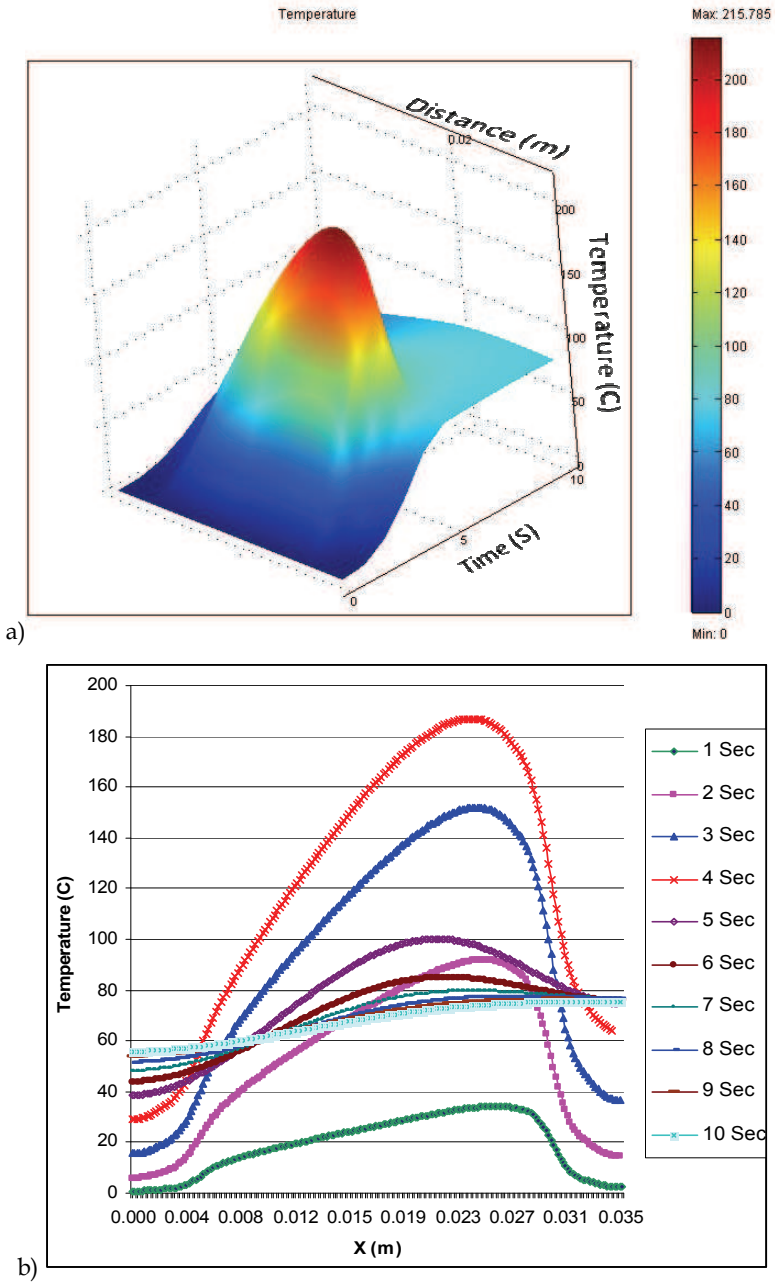


Figure 9. a) 3D temperature distribution during a 10 seconds time period. b) Temperature distribution plot at the different time steps

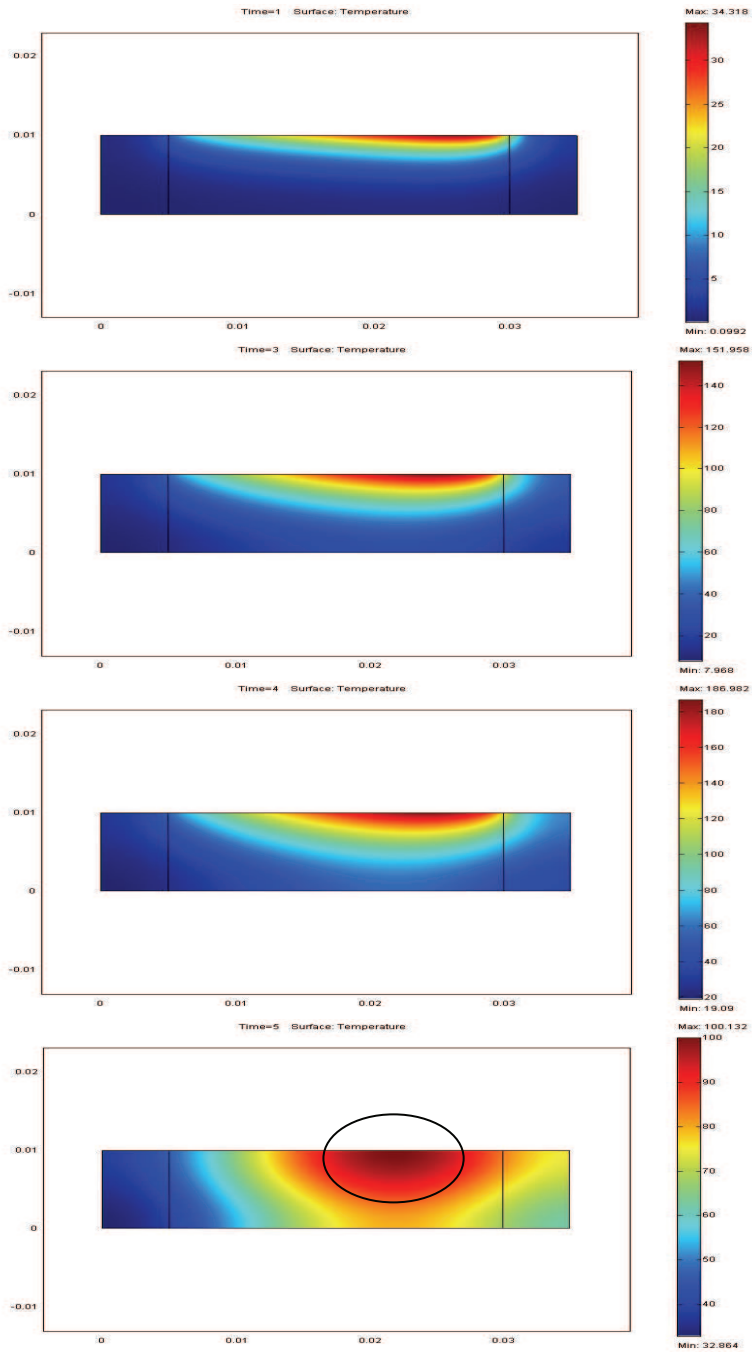


Figure 10. Change of the surface temperature across the disk brake, at time steps, 1, 3, 4, and 5s

A comparison between the temperature distributions produced during the braking process for the suggested different brake disk materials is shown in figure 11, as shown in the figure, the temperature distributions along the contact surface are plotted for the suggested disk materials, figure 11.a shows the temperature produced at an applied pressure of 4 MPa, while figure 11.b shows the temperature distribution produced at a pressure of 2 MPa.

From figures 11.a and b it can be concluded that both the Aluminum Metal Matrix composites and the ceramic brakes give better temperature distribution than the carbon-carbon composites. In other words, the Al-MMC's and the ceramic brakes provided evenly distributed temperature than the carbon-carbon composites, i.e. no localization of heat is expected compared to the carbon-carbon brakes.

In order to validate the proposed model and testing how accurate the model is, the maximum temperature obtained from the proposed model were compared to the actual measurement performed. A comparison was performed between the maximum temperature produced during the braking process using the proposed finite element analysis model and the actual measurements performed by Cueva et al. (2003), which is shown in table 1.

In their study, Cueva et al. measured the actual temperature produced during the braking process for 4 different types of iron, at different values of the applied pressure, as shown in the table a maximum difference of 10% between the calculated and the measured temperature was obtained. That percentage difference was considered as an accepted deviation between the simulated and the actual maximum temperature values produced.

	Actual temperature (°C) at 4MPa	Simulated temperature (°C)	Difference (%)	Actual temperature (°C) at 2MPa	Simulated temperature (°C)	Difference (%)
GI250	200 ±10	190	5	90 ±5	86	4.4
GIHC	210 ±10	189	10	85 ±5	82	3.5
GI250Ti	210 ±10	191	9	95 ±5	94	1
CGI	240 ±10	219	8.75	115 ±5	107	7

Table 1. comparison between the actual temperature measures by Cueva et al. and the simulated values obtained from the suggested finite element analysis model

Also, another comparison between two brake disk designs was conducted, in which the perforated and the notched disks were compared from the point of view of the temperature distribution and the heat flux as well. Figure 12 shows the temperature distributions for the two mentioned designs. Figure 12.a shows both the temperature distribution and the heat flux produced in the perforated disk brakes at time steps 4 and 10 s.

On the other hand, figure 12.b illustrates both the temperature distribution and the heat flux for the notched disk at the same time steps. As shown in Figure 12.a and b, both the perforated and the notched disks provided better results as far as the temperature distribution and the heat flux compared to the solid disk brakes, despite the fact that the maximum temperature produced is the same. It can be also concluded that the perforated disks gives better temperature distribution and heat flux compared to the notched ones.

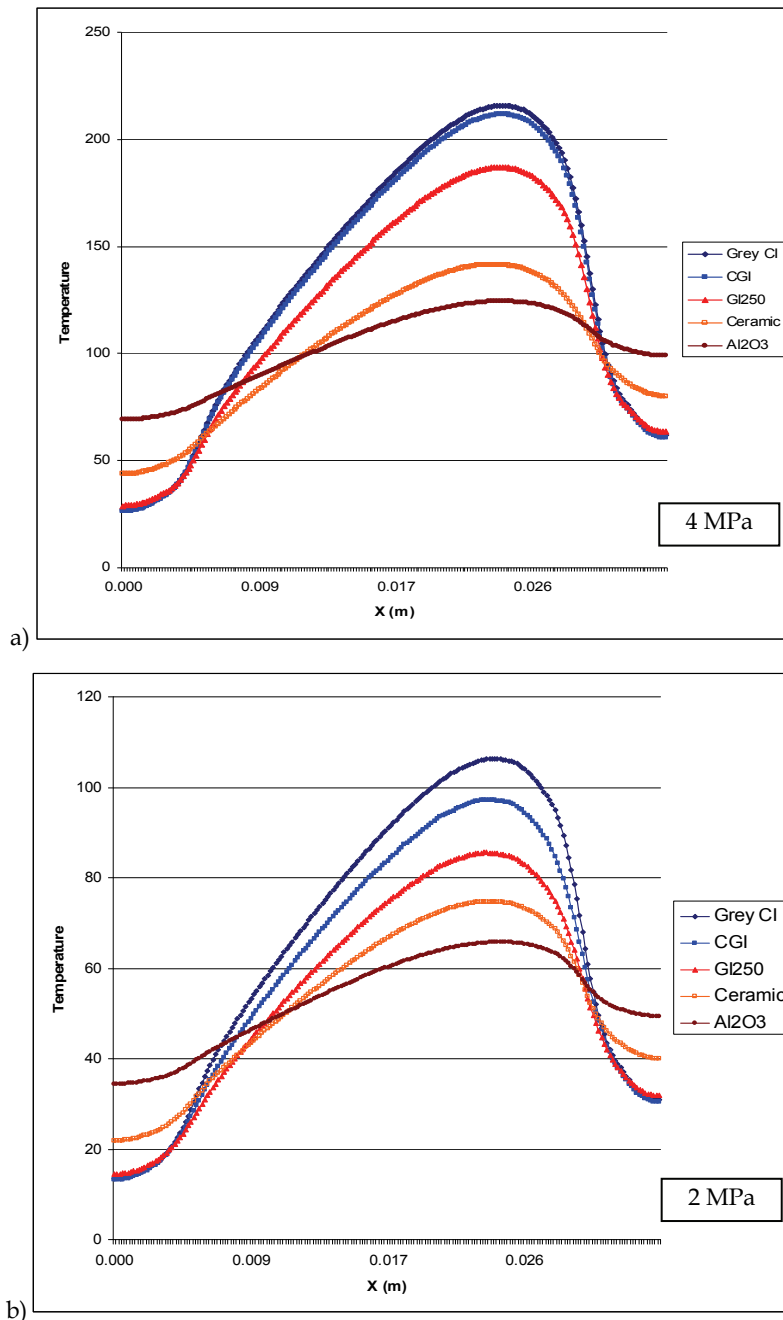


Figure 11. Comparison between the temperature distribution produced in Grey CI, CGI, GI250, Ceramic, and Al₂O₃ disk brakes at a pressure of a) 4MPa b) 2MPa

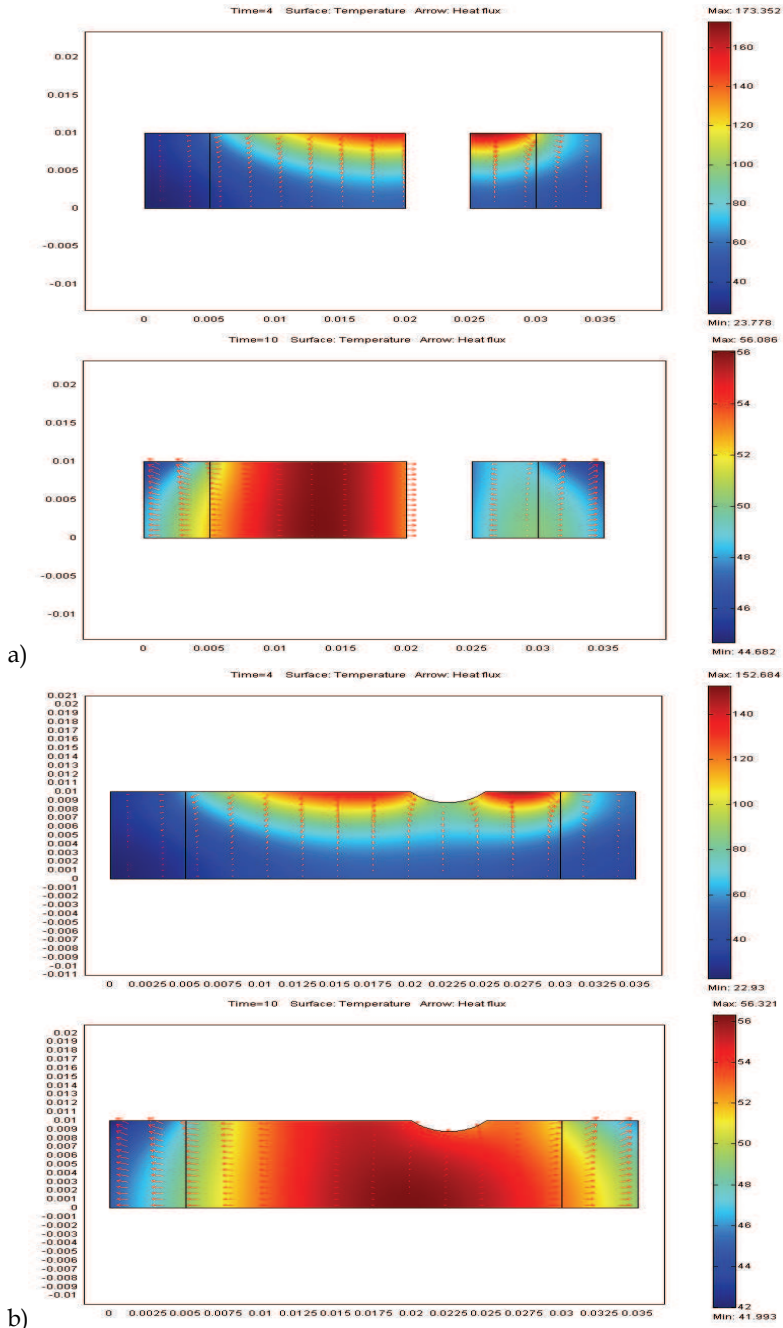


Figure 12. Comparison between the temperature distribution and the heat flux produce in a) the perforated disks b) the notched disks

4.4 Discussion

A finite element analysis model was developed in order to investigate both the thermal and mechanical behaviours taking place between the disk brake and the pad, during the braking process. The developed model was compared with actual measurements performed by Cueva et al. (2003) in order to validate the proposed model, and it showed very close simulated results compared to the actual ones. One of the obtained temperature distributions obtained during the braking action using the proposed model was compared to the one obtained by Choi et al. (2004) and it showed an excellent agreement.

The temperature distributions produced for five different disk's materials (Grey CI, CGI, GI250, Ceramic, and Al₂O₃) were compared to each other. Among the investigated materials, the ceramic and Al₂O₃ disk showed a better thermal behaviour during the braking process, as far as the maximum temperature and the temperature distribution produced, thus eliminating the localization of the produced heat, which means minimizing the probability of having hot spots.

Another comparison was performed between the perforated and the notched disks, in which the two designs were investigated under the same braking conditions. It was found that despite the fact that the maximum temperature produced in both was the same; the perforated disks produced better temperature distribution as well as heat flux as compared to notched disks.

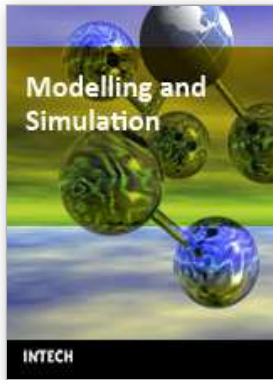
An interesting article by Kevin C. (2006), published at the New York Times, discussed the potential of the ceramics disk brakes and how that type of brakes represents the future of the disk brakes, he also mentioned a number of advantages that it possess, yet taking in to consideration the high cost of such rotor material. One of the advantages that the ceramic disk brake possesses is the outstanding hardness, the ability to maintain its strength and shape at extremely high temperature conditions, and more importantly it's considerably light in weight (almost half the weight of the conventional iron disk brakes).

One of the good reasons to consider the ceramic brakes is that they are light weight which will help reduce the weight of the vehicle which in turn will allow car manufacturers to meet the corporate average fuel economy standard (CAFE), which is now mandatory upon automakers. The importance of reducing the weight of the disk brakes in particular is because that as a vehicle accelerates, its rotating parts require more energy to accelerate than non rotating parts like engine blocks. This is because they gain energy from both their accelerating forward motion and from their increasingly rapid rotation and this gives brake discs a special importance in fuel economy.

5. References

- Abdelahamid, M. K. (1997). Brake judder analysis: Case studies, *SAE, Technical Paper Series*, no. 972027.
- Anderson, E., et al. (1990). Hot spotting in automotive friction systems, *Wear*, v. 135, pp. 319-337.
- Barber, J.R. (1967). The influence of thermal expansion on the friction and wear process, *Wear*, 10, 155-159.
- Barber, J.R. (1969). Thermoelastic instabilities in the sliding of conforming solids, *Proc. R. Soc. A* 312 381-394.
- Barber, R., J. et al. (1985). Implications of thermoelastic instabilities for the design of brakes, *Jnl. Tribology.*, v. 107, pp. 206-210.

- Choi, J.H. & Lee, I. (2003). Transient thermoelastic analysis of disk brakes in frictional contact, *Journal of Thermal Stresses*, 26, 223–244.
- Choi, J.H. & Lee, I. (2004). Finite element analysis of transient thermoelastic behaviors in disk brakes, *Wear*, 257, 47–58
- Cueva, G.; Sinatora, A.; Guesser, W.L. & Tschiptschin, A.P. (2003). Wear resistance of cast irons used in brake disk rotors, *Wear*, 255, 1256–1260
- De Vries, A. et al. (1992). The brake judder phenomenon, *SAE Technical Paper Series*, no. 920554.
- Dufrenoy, P. (2004). Two-/three dimensional hybrid model of the thermomechanical behavior of disc brakes, Proceedings of the Institution of Mechanical Engineers, *Journal of Rail and Rapid Transit*, 218, 17–30
- Eggleston, D. (2000). Thermal Judder, *EURAC Technical Bulletin*, 34056
- Eltoukhy, M.; Asfour, S.; Almakky, M. & Huang, C. (2006). Thermoelastic Instability in Disk Brakes: Simulation of the Heat Generation Problem, *Proceedings of the COMSOL Users Conference*, Boston
- Inoue, H. (1986). Analysis of brake judder caused by thermal deformation of brake discs, *SAE Technical Paper Series*, no. 865131.
- Jacobsson, H. (2003). Aspects of Disc Brake Judder, Proceedings of the Institution of Mechanical Engineers, *Journal of Automobile Engineering*, 217, 419–430
- Jang, J.Y. & Khonsari, M.M. (2003). A generalized thermoelastic instability analysis, Proceedings of the royal society, A459, 309–329
- Kennedy, F. E., & Ling, F. F. (1974). Thermoelastic, and Wear Simulation of a High-Energy Sliding Contact Problem, *Journal of Lubrication Technology*, 97, pp. 497–508.
- Kevin, C. (2006). Using Ceramics Brakes Are Light but Cost Is Heavy, *The New York Times journal*, published at: <http://www.nytimes.com/2006/06/18/automobiles/18BRAKES.html?pagewanted=2&r=1>
- Lee, K. (2000). Frictionally excited thermoelastic instability in automotive drum brakes, *ASME Journal of Tribology*, 122, 849–855
- Lee, K. & Brooks, F.W. (2003). Hot Spotting and Judder Phenomena in Aluminum Drum Brakes, *Transactions of the ASME*, 125, 44–51
- Rhee, K., S. et al. (1989). Friction-induced noise and vibration of disc brakes, *Wear*, v. 133, pp. 39–45.
- Sterne, D.D. (1989). Monitoring brake disc distortions using lasers, I.Mech.E. (Institution of Mechanical Engineers) *AUTOTECH '89 Conference*, Seminar paper C399/34.
- Zagrodzki, P. K.; Lam, B.; Al Bahkali, E. & Barber, J.R. (2001). Nonlinear transient behavior of a sliding system with frictionally excited thermoelastic instability, *Journal of Tribology*, 123, 699–708.



Modelling and Simulation

Edited by Giuseppe Petrone and Giuliano Cammarata

ISBN 978-3-902613-25-7

Hard cover, 688 pages

Publisher I-Tech Education and Publishing

Published online 01, June, 2008

Published in print edition June, 2008

This book collects original and innovative research studies concerning modeling and simulation of physical systems in a very wide range of applications, encompassing micro-electro-mechanical systems, measurement instrumentations, catalytic reactors, biomechanical applications, biological and chemical sensors, magnetosensitive materials, silicon photonic devices, electronic devices, optical fibers, electro-microfluidic systems, composite materials, fuel cells, indoor air-conditioning systems, active magnetic levitation systems and more. Some of the most recent numerical techniques, as well as some of the software among the most accurate and sophisticated in treating complex systems, are applied in order to exhaustively contribute in knowledge advances.

How to reference

In order to correctly reference this scholarly work, feel free to copy and paste the following:

M. Eltokhy and S. Asfour (2008). Braking Process in Automobiles: Investigation of the Thermoelastic Instability Phenomenon, *Modelling and Simulation*, Giuseppe Petrone and Giuliano Cammarata (Ed.), ISBN: 978-3-902613-25-7, InTech, Available from:

http://www.intechopen.com/books/modelling_and_simulation/braking_process_in_automobiles__investigation_of_the_thermoelastic_instability_phenomenon

INTECH

open science | open minds

InTech Europe

University Campus STeP Ri
Slavka Krautzeka 83/A
51000 Rijeka, Croatia
Phone: +385 (51) 770 447
Fax: +385 (51) 686 166
www.intechopen.com

InTech China

Unit 405, Office Block, Hotel Equatorial Shanghai
No.65, Yan An Road (West), Shanghai, 200040, China
中国上海市延安西路65号上海国际贵都大饭店办公楼405单元
Phone: +86-21-62489820
Fax: +86-21-62489821

© 2008 The Author(s). Licensee IntechOpen. This chapter is distributed under the terms of the [Creative Commons Attribution-NonCommercial-ShareAlike-3.0 License](#), which permits use, distribution and reproduction for non-commercial purposes, provided the original is properly cited and derivative works building on this content are distributed under the same license.